Droplet Velocity, Size, and Local Holdup Measurements in an Extraction Column by Tri-Sensor Optical Probe

Tingliang Xie, Yang Gao, and Wei Liu
Fundamental Science on Nuclear Safety and Simulation Technology Laboratory, College of Nuclear Science and Technology, Harbin Engineering University, Harbin 150001, China

DOI 10.1002/aic.14889
Published online June 8, 2015 in Wiley Online Library (wileyonlinelibrary.com)

The tri-sensor optical probe was applied to study the hydrodynamic characteristic in a pulsed sieve plate extraction column. Two immiscible liquids consisting of the dispersed phase (kerosene) and continuous phase (water) were introduced in countercurrent operation. Local parameters such as droplet velocity, drop size, and holdup of the dispersed phase were obtained. It was found that the tri-sensor optical probe could be used as an efficient and convenient technique for measuring local hydrodynamic parameters inside the pulsed sieve plate extraction column. Furthermore, the results indicated that pulsation intensity imposed more influence on these hydrodynamic parameters than two-phase superficial flow rates in the investigated ranges. Experimental results were found to be in good agreement with the empirical correlations reported in literature. © 2015 American Institute of Chemical Engineers *AIChE J*, 61: 3958–3963, 2015
Keywords: extraction column, local holdup, drop size, droplet velocity, tri-sensor optical fiber probe

Introduction

Liquid-liquid extraction is a technique for separating the components of a solution by distribution between two immiscible liquid phases. It is widely applied in petroleum, chemical, metallurgy pharmaceutical, food processing, biotechnology, and nuclear industries. As one of the most commonly used devices in extraction process, pulsed sieve plate extraction column offers large interfacial area, high mass transfer coefficient, high turbulence, therefore, it is of prime importance in spent fuel reprocessing process. Extensive work[1–4] has been carried out to study the hydrodynamic and mass-transfer characteristic in the pulsed sieve plate extraction column. Accurate prediction of dispersed phase droplet behavior is crucial to the design and scaling-up of the extraction column.

The knowledge of various dispersed phase properties such as droplet velocity, drop size, holdup of the dispersed phase, is of considerable importance for the proper design and scaling-up of extraction columns. For instance, droplet behaviors play key roles in determining the mass-transfer rate in extraction columns. Furthermore, drop-size distribution and droplet-velocity distribution are key parameters in evaluating the drag forces of two phases and using the population balance model in computational fluid dynamics (CFD). Many methods have been developed to measure all these parameters. Among these measurement techniques, conductivity[5] probe technique can only be applied to systems with a conductive dispersed phase and insulated continuous phase. Sampling[6,7] methods can destroy the two-phase flow field. In most cases, the laser scattering[8] and photographing[9] methods can only be applied to liquid-liquid two-phase flow systems with low holdup, although using an endoscope technique, it is also possible to take pictures inside columns for a large holdup.[10] In addition, double optical probe[11–14] and four-point optical probe[15,16] have been widely used in measuring liquid-liquid, gas-liquid local properties. However, double fiber probe cannot provide information about the angle of the droplet motion with respect to the vertical axis. Moreover, because of spiraling and zigzagging motions of the droplets, it is not sure that whether tips of two probes pierce the same droplet. Furthermore, the four-sensor optical probe has some disadvantages including complicated fabrication process and cumbersome data processing.

Recently, Yang et al[17] has measured two-dimensional (2-D) vapor bubble velocity with a tri-single-fiber-optical-probe technique, and the deviation between measured and the calculated vertical component of the velocity is within ±30%. In this article, a tri-sensor optical probe with data processing algorithm has also been used to investigate dispersed phase hydrodynamic characteristic in a pulsed sieve plate extraction column. Droplet properties, such as droplet velocity, drop size, the angle of the droplet motion, and local holdup of dispersed phase have been measured at various pulsation intensities and two-phase superficial velocities. The results can present data needed for CFD validation and engineering model.

Materials and Methods

Pulsed sieve plate extraction column

The schematic diagram of the pulsed sieve plate extraction column is shown in Figure 1. The internal diameter of the extraction column is 0.038 m, and active height is 1.474 m. The column is fitted with regularly spaced (0.05 m) sieve plates mounted on a rod of 0.006 m at the center of the column. Each sieve contains 32 circular holes of 0.003 m

Correspondence concerning this article should be addressed to Y. Gao at gaoyang@hrbeu.edu.cn.

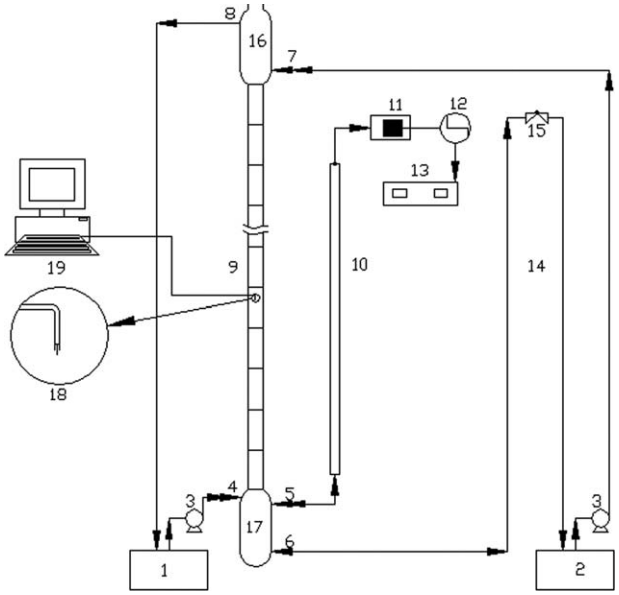

Figure 1. A schematic of the pulsed sieve plate extraction column.

1. light phase feed vessel, 2. heavy phase feed vessel, 3. peristaltic pump, 4. light phase inlet, 5. Pulse inlet, 6. heavy phase outlet, 7. heavy phase inlet, 8. light phase outlet, 9. extraction section, 10. pulse leg, 11. air cylinder, 12. stepper motor, 13. digital regulator, 14. balance leg, 15. Vent, 16. up separating chamber, 17. down separating chamber, 18. Probe, 19. A/D unit and computer.

diameter, which can assist to increase the interfacial area between the immiscible liquids by breaking the droplets of dispersed phase. Two settlers are located at each end of the contactor to facilitate the separation of phases after their contact in the column body. An air pulsation was used for the liquid in the column. A pulse leg of 0.016-m diameter and 1.624 m in length was connected at the base of bottom disengaging section for pulsing the continuous phase. The air pressure was controlled by digital regulator and stepper motor to provide pulses with different frequencies and a fixed amplitude of 0.055 m. The frequency of the pulse was varied with the rotation speed of the stepper motor. The two phases were introduced countercurrently into the column through circular perforated distributors with the light phase entering from the bottom while heavy phase from the top. The distributor contains eight circular holes of 0.003-m diameter, which can assist to produce the droplets of 0–0.003-m diameter.

Water and kerosene were taken as the continuous phase and dispersed phase, respectively. Physical properties of two phases are shown in Table 1. The interfacial tension was measured with a BZY-2 tensiometer and viscosities were measured with a NDJ-8S viscometer.

Description of the probe measurement system

As shown in Figure 1, the tri-sensor probe was placed at between the 13th and 14th stainless steel plates from the bottom of the active section with its sensor tips facing vertically downward, well away from the dispersed phase inlet. The tips of the tri-sensor probe located in a middle height in this compartment. As Figure 2a shows, each fiber is consisted of three layers: a quartz glass core of 0.125-mm diameter having a refraction index of 1.48, a silicon cladding of 0.9-mm diameter, and a protective layer of Teflon of 3-mm diameter. As Figure 2b illustrates, the distance between each tip of the sensors was adjusted to approximately 1 mm (e.g., $L_{12} = 1$ mm, $L_{13} = 1$ mm, $L_{23} = 1$ mm), and the values for angle1, angle2, and angle3 were all $\pi/3$.

Table 1. Physical Properties of Kerosene/Water

Parameters	Water	Kerosene
Density of the phase (kg/m^3)	998	803
Viscosity of the phase (mPa s)	1.0	1.66
Interfacial tension (N/m)	0.0444	

The light emitted from a laser light source is transmitted through an optical fiber to the probe and is reflected at the sensor tip. The reflected light backtracks to a probe signal processor, which can convert light signals to corresponding electric signals.

Measurement principle of tri-sensor probe

In this water-kerosene system, the core refractive index of silica fiber is 1.48, and the theoretical reflection coefficients of the water phase (the refractive index is 1.33) and the kerosene phase (the refractive index is 1.44) can be calculated according to Eq. 1

$$R = \left(\frac{n_0 - n}{n_0 + n}\right)^2 \tag{1}$$

where R denotes the reflection coefficient, n_0 is the core refractive index, and n stands for the refractive indexes of the two phases.

The difference in refractive indices of the two liquids allows the probe tips to differentiate the light intensities reflected from the two passing phases. Then the dispersed phase properties can be derived by processing the response with an appropriate algorithm.

The data processing algorithm for tri-sensor probe measurement

Here the data processing algorithm includes five steps: (1) single threshold signal processing; (2) estimating the local holdup; (3) eliminating uncorrelated signals; (4) solving the droplet velocity and direction angle θ (the angle of the droplet motion with respect to the vertical axis); and (5) calculating droplet diameter.

Single threshold signal processing

Due to the effect of surface tension of droplets, there exists a time delay when the tips pierce the droplets and leave the

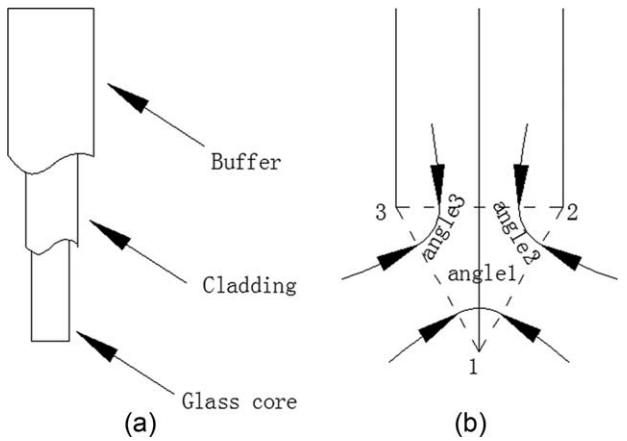

Figure 2. Optical fiber probe

(a) schematic of the optical fiber, (b) a picture of the tri-sensor optical fiber probe.

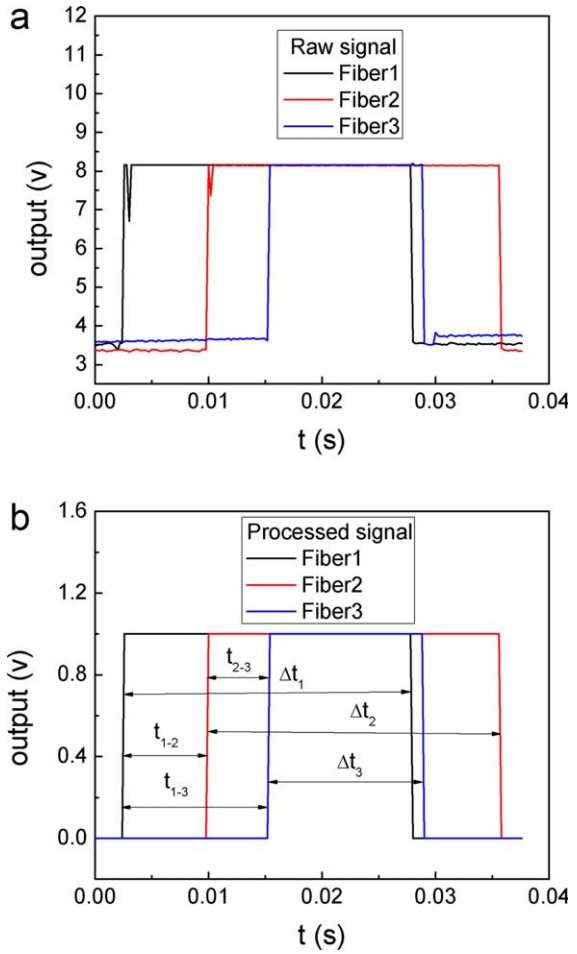

Figure 3. Illustration of the raw signal (a) and the processed signal (b).

[Color figure can be viewed in the online issue, which is available at wileyonlinelibrary.com.]

droplets. In addition, because of the interference originating from the internal measurement system and the external environment, the signal output from the optical probe is different from the ideal two-state square-wave. To facilitate subsequent data processing, threshold methods proposed by Barrau et al.[11] and Yuan et al.[16] were used to process the raw probe signals and extract the required information from the two phases. The raw signal obtained by the aforementioned method as well as the processed signal from a tri-sensor probe is displayed in Figure 3, in which the high and low voltages represent the dispersed phase and continuous phase, respectively.

Measurement of local holdup

The local holdup obtained by the optical probe is reliable, which has been proved by Hamad et al.[13] and Xue et al.[18] Based on the recorded signal information from a tri-sensor probe, the local holdup ϕ obtained by probe tip-1 (the 1st probe tip) is defined as Eq. 2

$$\phi=\frac{\text{Time spent by the probe tip-1 in droplets}}{\text{Total measurement time}}=\frac{T_1}{T_t} \quad (2)$$

Elimination of uncorrelated signals

To increase the accuracy for measuring droplet diameter and droplet velocity, correlation principle[17] and pulse width comparison methods[19] are taken to eliminate. uncorrelated signals. The selected signals of droplets should satisfy that not only all the three probe tips penetrate the same droplet but also any tip of three probes cannot just penetrate the edge of the droplet, and Yang et al.[17] has describe the method of eliminating uncorrelated signals in detail.

Measurement of the drop velocity (v) and direction angle (θ)

With this data processing algorithm, there is no need for selecting only a specific population of droplets (e.g., drops moving in the probe's axial direction). Instead, the whole droplet population can be used to determine the hydrodynamic characteristic of the disperse phase.

Figures 4a, b show the schematic when a droplet hits the tri-sensor optical probe. Yang et al.[17] has described the solving method of the migration distance (L_{2c}, L_{3b}), the droplet chord lengths (L_{1i}, L_{cj}, L_{bh}), and direction angle (θ) in detail.

Obviously, there are two cases involved in estimating the new values of L_{2c}, L_{3b} (represented as L_{2c}^*, L_{3b}^*, respectively). If $L_{3d}>0$, L_{2c}^* is described as Eq. 3 and Eq. 4. If $L_{3d}<0$, L_{3b}^* can be described as Eqs. 5 and 6 and then repeat iteration method can be used to calculate the final velocity u. Simultaneously the migration distance (L_{2c}, L_{3b}), the droplet chord length (L_{1i}, L_{cj}, L_{bh}), and the direction angle θ can also be determined

$$L_{2c}{}^*=\cos(\pi/2+\theta-\text{angle2})\times L_{12}+0.5L_{1i}-0.5L_{cj} \quad (3)$$

$$L_{2c}{}^*=t_{1-2}\times u \quad (4)$$

$$L_{3b}{}^*=\cos(\pi/2+\theta-angle3)\times L_{13}+0.5L_{1i}-0.5L_{bh} \quad (5)$$

$$L_{3b}{}^*=t_{1-3}\times u \quad (6)$$

where u denotes the new droplet velocity.

Measurement of droplet diameter

If $L_{3d}>0$, droplet diameter is estimated as Eq. 7. If $L_{3d}<0$, droplet diameter can be estimated as Eq. 8 and Sauter droplet diameter is estimated as Eq. 9

$$\sqrt{(0.5d)^2-(0.5L_{bh})^2}-\sqrt{(0.5d)^2-(0.5L_{1i})^2}=L_{13}\times\sin(\pi/2-\theta-\text{angle3}) \quad (7)$$

$$\sqrt{(0.5d)^2-(0.5L_{cj})^2}-\sqrt{(0.5d)^2-(0.5L_{1i})^2}=L_{12}\times\sin(\pi/2-\theta-\text{angle2}) \quad (8)$$

$$d_{32}=\frac{\sum_{i=1}^{n}n_i d_i{}^3}{\sum_{i=1}^{n}n_i d_i{}^2} \quad (9)$$

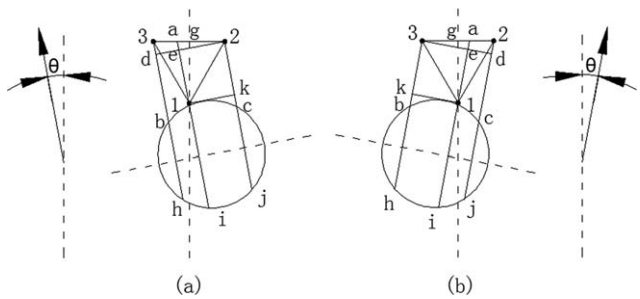

Figure 4. Schematic of the probe piercing the droplet.

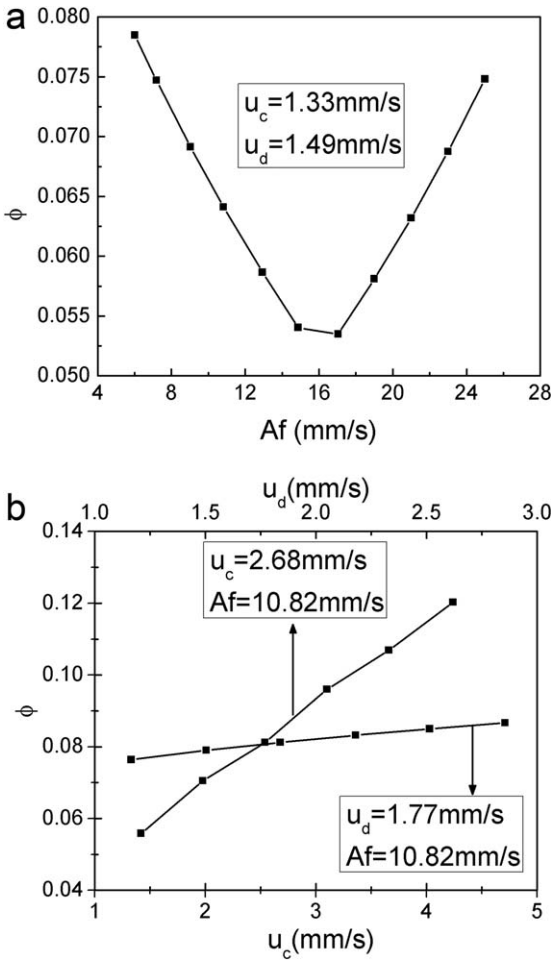

Figure 5. Local holdup variation with pulsation intensity (a), two-phase superficial velocity (b).

where d_{32} is the Sauter droplet diameter, and d_i (mm) is the ith drop diameter, and n and i represent nth and ith values, respectively. It should be noticed that due to the arrangement configuration of the three probe tips, there is a minimum measureable droplet size of 1.03 mm through a simple geometrical deduction.

Results and Discussion

Local holdup

The effect of pulsation intensity on local hold up (ϕ) is displayed in Figure 5a. Dispersed phase holdup decreases with an increase in low pulsation intensity, and attains a minimum value, beyond which it increases with an increase in pulsation intensity. The variation is consistent with the observations reported in literature for the liquid pulsed column.[20] The results shown in Figure 5b indicate that local holdup increases with an increase in continuous phase superficial velocity. The most probable explanation of this behavior is that the drag force between the dispersed droplets and the continuous phase increases, so the droplet movement will be limited and the residence time will increase. In addition, Figure 5b illustrates that the local holdup increases with an increase in dispersed phase superficial velocity. The number of the dispersed droplets increases with an increase in dispersed phase superficial velocity, which will increase the holdup of the dispersed phase.

Droplet mean velocity

The result shown in Figure 6a indicates a decrease in droplet velocity with the increase in pulsation intensity. Droplet diameter will be smaller because of more turbulence generated at the higher pulse energy, consequently, droplet velocity decreases. Figure 6b shows droplet velocity is practically independent of the continuous superficial velocity for the range of conditions investigated, however, droplet velocity decreases significantly with an initial increase in the dispersed superficial velocity, while it seems not to be affected at higher velocity values. Furthermore, droplet velocities are more sensitive to changes in pulsation intensity than dispersed superficial velocity.

Accurate prediction of dispersed phase droplet velocity is very difficult for the lack of effective experimental technology, so rare experiment data, and empirical correlations can be found in the published literature. Typically, the characteristic velocity is used as the real droplet velocity. Zhu et al.[21] put forward the following correlation (10) for calculation of characteristic velocity in a pulsed sieve plate extraction column, in which the internal diameter of the column is 41 mm, and four physical systems have been considered. The comparison of the experimental results with those predicted by Eq. 10 is illustrated in Figure 7, the relative deviation is within 25%

$$V_0 = 0.447\left(\frac{3\mu_d + 3\mu_c}{3\mu_d + 2\mu_c}\right)^{2.75}\left(\frac{\Delta\rho}{\rho_c}\right)^{2/3}\left(\frac{\rho_c}{\mu_c}\right)^{1/3} d_{32} \qquad (10)$$

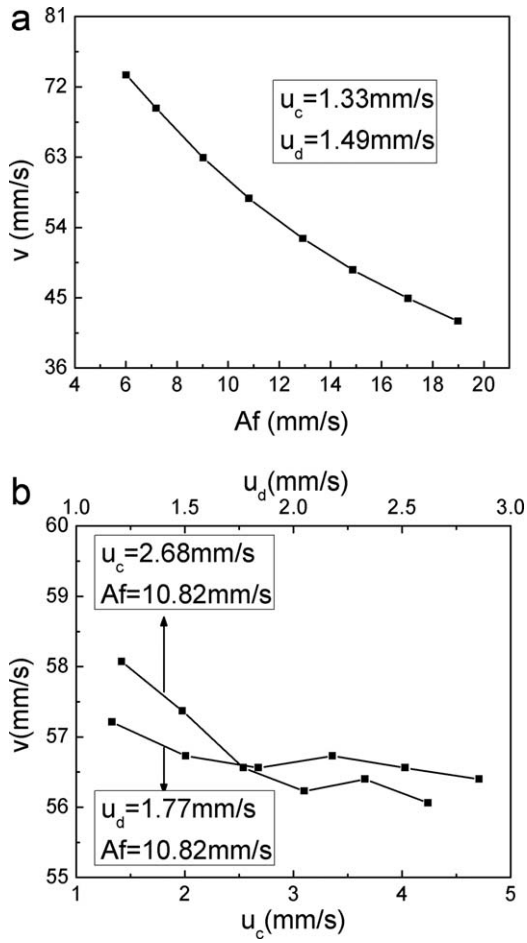

Figure 6. Droplet velocity variation with pulsation intensity (a), two-phase superficial velocity (b).

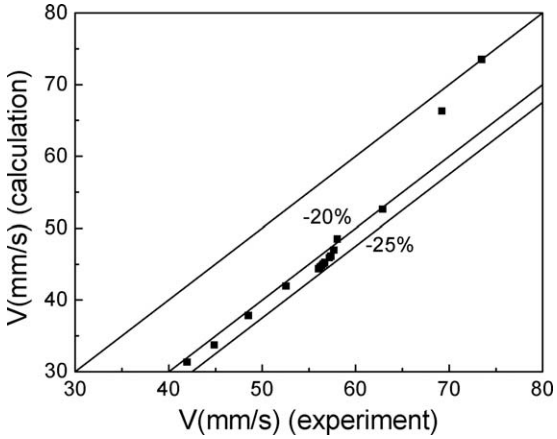

Figure 7. Comparison of the experimental and calculated droplet velocity.

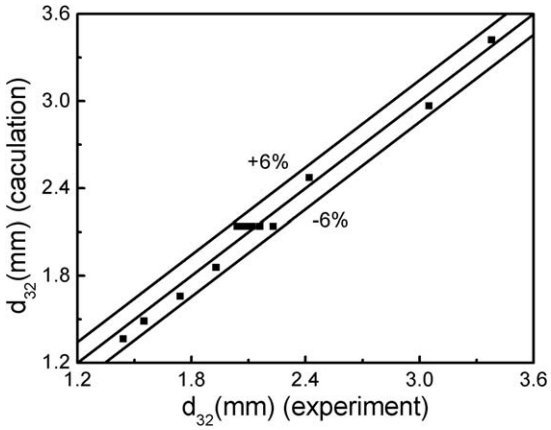

Figure 9. Comparison of the experimental and calculated droplet Sauter diameter.

where V_0 is the characteristic velocity, μ_c is the viscosity of continuous phase, μ_d is the viscosity of dispersed phase, $\Delta\rho$ is the density difference between two phases, and ρ_c is the density of continuous phase.

Drop mean diameter

The influence of pulsation intensity and two-phase superficial velocity on Sauter droplet diameter d_{32} is shown in Figure 8. Figure 8a illustrates that d_{32} decreases with an increase in pulsation intensity as it is expected, because more turbulence generates at the higher pulse energy. Also, it is observed that this decrease in droplet diameter is more pronounced at the lower pulsation intensities than higher pulsation intensities. As showed in Figure 8b, continuous phase superficial velocities have a much smaller effect on d_{32} at constant pulsation intensity and dispersed phase superficial velocity. In addition, Figure 8b reveals the facts that in the lower dispersed phase superficial velocity region, d_{32} sharply decreases with the increase of the dispersed phase superficial velocity, while much smaller influence can be found on droplets diameter in higher dispersed phase superficial velocity. The comparison of Figures 8a, b shows that pulsation intensity has much more significant effects on droplet diameter than two-phase superficial velocity in the investigated ranges.

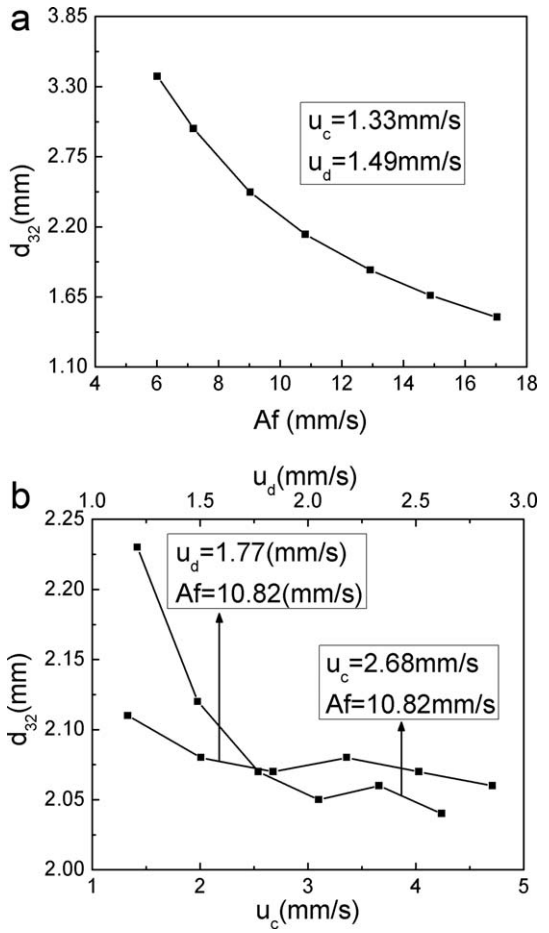

Figure 8. Sauter droplet diameter variation with pulsation intensity (a), two-phase superficial velocity (b).

A large number of empirical correlations[22–24] have been presented for calculating the droplet Sauter diameter in the past literatures. For example, Sreenivasulu et al.[23] has measured droplet Sauter diameter by photographing methods in 0.043-m diameter column, in which kerosene was used as the dispersed phase, and water was the continuous phase. They presented the following correlation (11) for calculating droplet Sauter diameter in pulsed column. This correlation has been also recommended for the design and scaling-up of pulsed sieve plate columns by Yadav and Patwardhan[24] The comparison between our results and calculated drop Sauter diameter through the correlation (11) is described in Figure 9, and it can be found that the related deviation is within $\pm 6\%$

$$d_{32} = C\left(\frac{\sigma}{\rho_c}\right)^{0.4} (Af)^{-0.8} \alpha^{0.48} d^{0.26} h^{0.34} \tag{11}$$

where the constant $C = 2.0 \times 10^4$, α denotes the fractional free area, d is the hole diameter, and h is the plate spacing.

Conclusions

Hydrodynamic characteristic of a liquid-liquid two-phase system was studied by means of tri-sensor optical probe in a pulsed sieve plate extraction column, in which the continuous phase was water and the dispersed phase was kerosene. The local hydrodynamic parameters including droplet velocity, drop size, and holdup of the dispersed phase were determined accurately and conveniently. The results indicate that the local holdup of the dispersed phase increases with an increase in two-phase superficial velocity, while decreases with an increase in low pulsation intensity, attains a minimum value, beyond which

it increases with an increase in pulsation intensity. Both the mean droplet velocity and the Sauter mean diameter decrease with an increase in pulsation intensity and dispersed phase superficial velocity, however, are practically independent of the continuous phase superficial velocity. The experimental droplet velocity and drop size of the dispersed phase are in good agreement with the empirical correlations reported in literature. The relative deviation between the experimental droplet velocity and the calculated value of the empirical correlation is within 25%. The experimental droplet Sauter diameter has be compared with the Sreenivasulu's correlation, and the related deviation is within $\pm 6\%$ in general. It is demonstrated that tri-sensor fiber optical probe can be effectively applied to the liquid-liquid two-phase flow measurement.

Acknowledgment

The work was supported by Special Fund of Central University Basic Scientific Research Fee (HEUCF141503).

Literature Cited

1. Tung LS, Luecke RH. Mass transfer and drop size in pulsed-plate extraction columns. *Ind Eng Chem Process Des Dev*. 1986;25:664–673.
2. Luo GS, Li HB, Fei WY, Wang JD. A simplified correlation of mass transfer in a pulsed sieve plate extraction column. *Chem Eng Technol*. 1998;21:823–827.
3. Din GU, Chughtai IR, Inayat MH, Khan IH. Study of axial mixing, holdup and slip velocity of dispersed phase in a pulsed sieve plate extraction column using radiotracer technique. *Appl Radiat Isotopes*. 2009;67:1248–1253.
4. Lade VG, Pakhare AD, Rathod VK. Mass transfer studies in pulsed sieve plate extraction column for the removal of tributyl phosphate from aqueous nitric acid. *Ind Eng Chem Res*. 2014;53:4812–4820.
5. Moris MA, Diez FV, Coca J. Hydrodynamics of a rotating disc contactor. *Sep Purif Technol*. 1997;11:79–22.
6. Kentish SE, Stevens GW, Pratt HRC. Estimation of coalescence and breakage rate constants within a kuhni column. *Ind Eng Chem Res*. 1998;37:1099–1106.
7. Steiner L, Balmelli M, Hartland S. Simulation of hydrodynamic performance of stirred extraction column. *AIChE J*. 1999;45:257–267.
8. Simmons MJH, Azzopardi BJ. Drop size distributions in dispersed liquid-liquid pipe flow. *Int J Multiphase Flow*. 2001;27:843–859.
9. Tsouris C, Kirou VI, Tavlarides LL, Wang CY. Drop size distribution and holdup profiles in a multistage extraction column. *AIChE J*. 1994;40:407–418.
10. Maaß S, Wollny S, Voigt A, Kraume M. Experimental comparison of measurement techniques for drop size distributions in liquid/liquid dispersions. *Exp Fluids*. 2011;50:259–269.
11. Barraua E, Rivièrea N, Poupotb CH, Cartelliera A. Single and double optical probes in air-water two-phase flows: real time signal processing and sensor performance. *Int J Multiphase Flow*. 1999;25:229–256.
12. Tang XJ, Luo GS, Wang JD. Optical probe technique for two-phase flow measurements in an extraction column. *AIChE J*. 2005;51:1565–1568.
13. Hamad FA, Pierscionek BK, Bruun HH. A dual optical probe for volume fraction, drop velocity and drop size measurements in liquid-liquid two-phase flow. *Meas Sci Technol*. 2000;11:1307–1318.
14. Richard K, Manson P, Ewart P. An optical probe for measurements in liquid-liquid two-phase flow. *Meas Sci Technol*. 1997;8:1122–1132.
15. Xue JL, Al-Dahhan M, Dudukovic MP, Mudde RF. Bubble velocity, size, and interfacial area measurements in a bubble column by four-point optical probe. *AIChE J*. 2008;54:350–363.
16. Yuan Z, Milorad PD, Muthanna HAD, Hui L. Multiphase hydrodynamics and distribution characteristics in a monolith bed measured by optical fiber probe. *AIChE J*. 2014;60:740–748.
17. Yang RC, Zheng RC, Zhou FL, Liu RL. Measurement of two-dimensional bubble velocity by using tri-fiber-optical probe. *J Phys: Conf Ser IOP Publ*. 2009;147:012028.
18. Xue JL, Al-Dahhan M, Dudukovic MP, Mudde RF. Four-point optical probe for measurement of bubble dynamics: validation of the technique. *Flow Meas Instrum*. 2008;19:293–300.
19. Lu YS, Zhang JM. Electronic Measurement of Two-Phase Flow Characteristic Parameters. JiNan: Shandong Science and Technology Press, 1989.
20. Lorenz M, Haverland H, Vogelpohl A. Fluid dynamics of pulsed sieve plate extraction columns. *Chem Eng Technol*. 1990;13:411–422.
21. Zhu SH, Zhang BQ, Shen ZY, Wang JD. A Study on two-phase characteristics in pulsed sieve plate column for liquid-liquid extraction column. *J Chem Ind Eng (China)*. 1982;1:1–14.
22. Kumar A, Hartland S. Prediction of drop size in pulsed perforated-plate extraction columns. *Chem Eng Commun*. 1986;44:163–182.
23. Sreenivasulu K, Venkatanarasaiah D, Varma YBG. Drop size distributions in liquid pulsed columns. *Bioprocess Eng*. 1997;17:189–195.
24. Yadav RL, Patwardhan AW. Design aspects of pulsed sieve plate columns. *Chem Eng J*. 2008;138:389–415.

Manuscript received Sep. 16, 2014, and revision received Apr. 22, 2015.